

Electronic Supplementary Information for  
**Synthesis mechanism and gas-sensing application of  
nanosheet-assembled tungsten oxide microspheres†**

**Shouli Bai,<sup>a</sup> Kewei Zhang,<sup>a</sup> Liangshi Wang,<sup>b</sup> Jianhua Sun,<sup>ac</sup> Ruixian Luo,<sup>\*a</sup> Dianqing  
Li<sup>\*a</sup> and Aifan Chen<sup>a</sup>**

<sup>a</sup> State Key Laboratory of Chemical Resource Engineering, Beijing University of  
Chemical Technology, Beijing 100029 China

<sup>b</sup> National Engineering Research Center for Rare Earth Materials, General Research  
Institute for Nonferrous Metals, and Griem Advanced Materials Co. Ltd., Beijing  
100088, China

<sup>c</sup> Guangxi Key Laboratory of Petrochemical Resource Processing and Process  
Intensification Technology, School of Chemistry and Chemical Engineering, Guangxi  
University, Nanning 530004, China

\*Corresponding author:  
Tel.: + 86 010 64961040  
E-mail: luorx@mail.buct.edu.cn

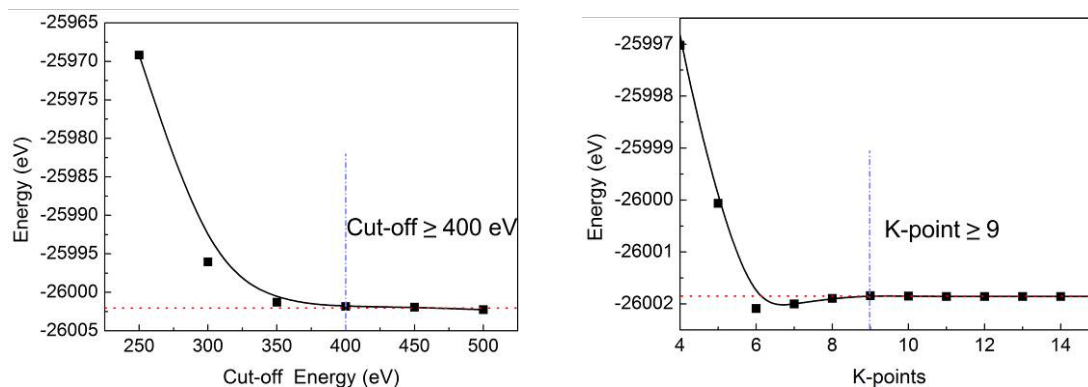


**Fig. S1** Energy convergence of bulk  $\text{WO}_3$  with increasing plane wave cut-off energy (left) and number of k-points (right).

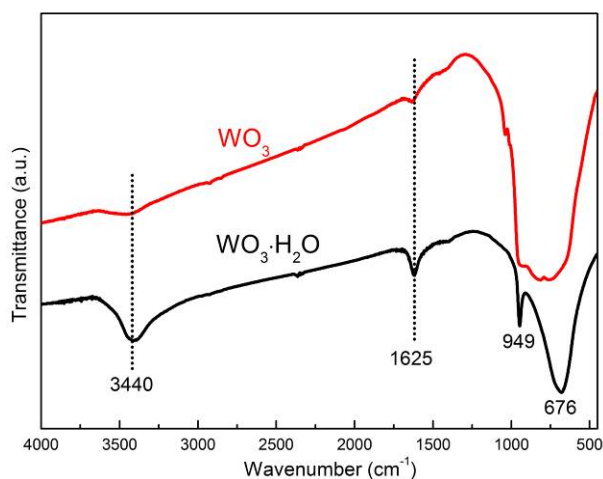


**Fig. S2** FT-IR spectra of the  $\text{WO}_3 \cdot \text{H}_2\text{O}$  and  $\text{WO}_3$  samples.

Fig. S2 shows the FT-IR spectra of the  $\text{WO}_3 \cdot \text{H}_2\text{O}$  and  $\text{WO}_3$  samples. The FT-IR spectrum of as-synthesized  $\text{WO}_3 \cdot \text{H}_2\text{O}$  shows a broad band in the range 3000-3700  $\text{cm}^{-1}$ , which can be assigned as O-H stretching vibrations of the adsorbed water. The peaks located at 1625  $\text{cm}^{-1}$  is indexed to O-H bending modes of the adsorbed water. Below 1000  $\text{cm}^{-1}$ , the FT-IR spectrum shows a small and sharp peak at 949  $\text{cm}^{-1}$ , assigned as the stretching of short W=O bonds of  $\text{WO}_3 \cdot \text{H}_2\text{O}$ . The broad band around 676  $\text{cm}^{-1}$  is attributed to the stretching of O-W modes. The absence of carbonyl peak around 1730  $\text{cm}^{-1}$  indicates removing of oxalate during the washing process. For the annealed  $\text{WO}_3$  sample (red line), the hydrogen bonded W-OH groups show a large

decrease due to dehydration of  $\text{WO}_3 \cdot \text{H}_2\text{O}$ . The broad absorption peaks in the range 500–1000  $\text{cm}^{-1}$  are characteristic of the different O-W-O stretching vibrations in the  $\text{WO}_3$  crystal lattice.

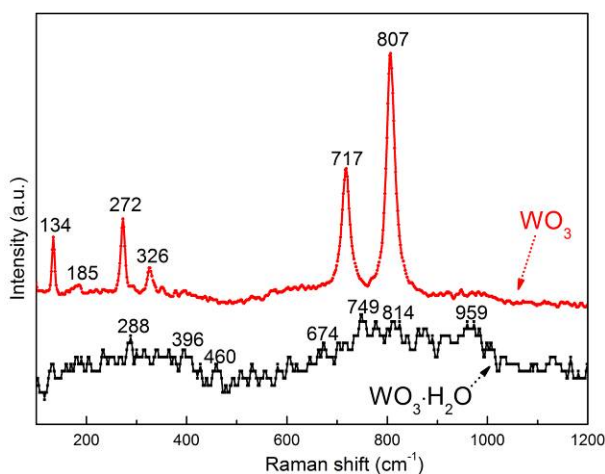


**Fig. S3** Raman spectra of the  $\text{WO}_3 \cdot \text{H}_2\text{O}$  and  $\text{WO}_3$  samples.

The structural defects and disorders of the samples are further identified by Raman spectra, as shown in Fig. S3. For the  $\text{WO}_3 \cdot \text{H}_2\text{O}$  sample, two characteristic Raman peaks of  $\text{WO}_3 \cdot \text{H}_2\text{O}$  at 959 and 674  $\text{cm}^{-1}$  are observed. The band situated at 959  $\text{cm}^{-1}$  is attributed to the symmetric stretching mode of terminal (W=O) groups; this mode is common for all types of tungsten trioxide hydrates. The peak observed at 674  $\text{cm}^{-1}$ , which can be attributed to stretching modes arising from W-OH<sub>2</sub>, is consistent with the presence of  $\text{WO}_3 \cdot \text{H}_2\text{O}$  phases. The weak transitions at 460  $\text{cm}^{-1}$  may be associated with water librations. After annealing, the peaks at 959 and 674  $\text{cm}^{-1}$  almost disappear, while six well-defined peaks arising from  $\text{WO}_3$  phase (134, 185, 272, 326, 717 and 807  $\text{cm}^{-1}$ ) can be observed. This indicates that  $\text{WO}_3 \cdot \text{H}_2\text{O}$  has completely transformed into monoclinic  $\text{WO}_3$  after annealing, and the particle size and crystallinity increase. As is reported in the literatures,  $\text{WO}_3$  consists of network of corner-sharing  $\text{WO}_6$  octahedron units which are capable of forming clusters. The crystalline clusters are

supposed to be connected to each other by W-O-W. The peaks at 807 and 717  $\text{cm}^{-1}$  are assigned as the stretching of W-O-W, in which the longer W-O-W bonds are responsible for the stretching mode at 717  $\text{cm}^{-1}$  and the shorter W-O-W bonds are the source of the 807  $\text{cm}^{-1}$  peak. The peaks at 272 and 326  $\text{cm}^{-1}$  are assigned to the W-O-W bending vibrations of bridging oxygen, whereas those observed at 134 and 185  $\text{cm}^{-1}$  belong to the lattice vibration of crystalline  $\text{WO}_3$ .

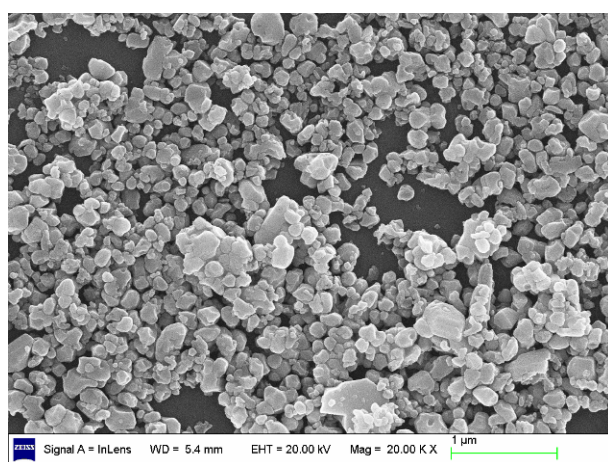


**Fig. S4** FESEM micrograph of commercial  $\text{WO}_3$  powder.

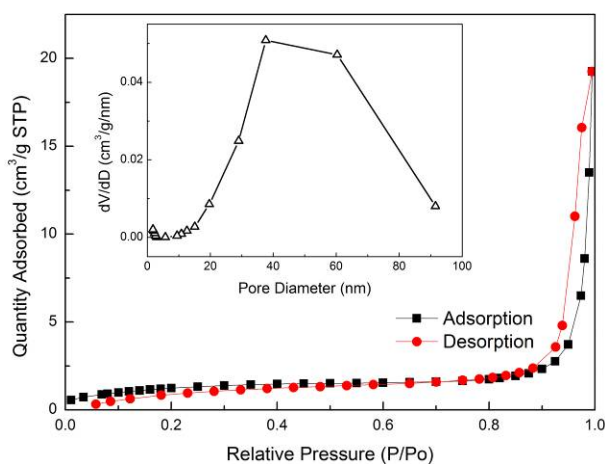


**Fig. S5**  $\text{N}_2$  adsorption-desorption isotherm and the corresponding pore size

distribution (inset) of commercial  $\text{WO}_3$  particles.

The commercial  $\text{WO}_3$  particles exhibit type-III pattern of isotherm with H4 hysteresis loop, in which the two branches are almost vertical and nearly parallel over an appreciable range of relative pressure. The BET surface area was determined to be  $4.8 \text{ m}^2\cdot\text{g}^{-1}$ , comparatively lower than that of hierarchical  $\text{WO}_3$  ca.  $12.8 \text{ m}^2\cdot\text{g}^{-1}$ . The result is in accordance with the gas-sensing measurements.

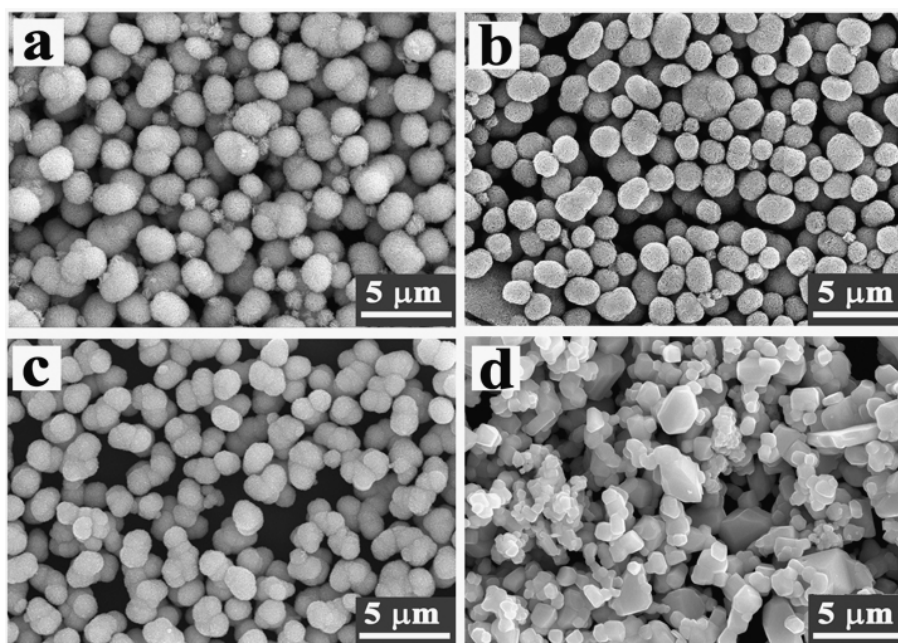


**Fig. S6** FESEM micrographs of (a) as-synthesized hierarchical  $\text{WO}_3\cdot\text{H}_2\text{O}$  and anhydrous hierarchical  $\text{WO}_3$  after annealing at (b) 500°C, (b) 700°C and (b) 900°C.

High annealing temperature, such as 900°C, would lead to breakage of the hierarchical morphology of  $\text{WO}_3$ . However, there would be no obvious change in morphology at low annealing temperatures, such as 500°C.